

Key Points:

- Northeast Greenland Winter Water is fresher than in the 1990s
- The cold halocline layer is a brine-enhanced mixture of river discharge and Atlantic Water
- The river discharge is primarily sourced from the Laptev Sea

Correspondence to:

E. W. Willcox,
willcox@myumanitoba.ca

Citation:

Willcox, E. W., Bendtsen, J., Mortensen, J., Mohn, C., Lemes, M., Pedersen, T.-J., et al. (2023). An updated view of the water masses on the Northeast Greenland shelf and their link to the Laptev Sea and Lena River. *Journal of Geophysical Research: Oceans*, 128, e2022JC019052. <https://doi.org/10.1029/2022JC019052>

Received 1 JUL 2022

Accepted 29 MAR 2023

© 2023 The Authors.

This is an open access article under the terms of the [Creative Commons Attribution-NonCommercial License](#), which permits use, distribution and reproduction in any medium, provided the original work is properly cited and is not used for commercial purposes.



An Updated View of the Water Masses on the Northeast Greenland Shelf and Their Link to the Laptev Sea and Lena River

E. W. Willcox¹ , J. Bendtsen² , J. Mortensen³ , C. Mohn⁴ , M. Lemes¹, T.-J. Pedersen³ , J. Holding^{4,5} , E. F. Møller^{4,5} , M. K. Sejr^{4,5}, M.-S. Seidenkrantz^{5,6,7} , and S. Rysgaard^{1,5} 

¹Centre for Earth Observation Science, CHR Faculty of Environment Earth, and Resources, University of Manitoba, Winnipeg, MB, Canada, ²Globe Institute, University of Copenhagen, Copenhagen, Denmark, ³Greenland Climate Research Centre, Greenland Institute of Natural Resources, Nuuk, Greenland, ⁴Department of Ecoscience, Aarhus University, Roskilde, Denmark, ⁵Arctic Research Centre, Department of Biology, Aarhus University, Aarhus, Denmark, ⁶Department for Geoscience, Aarhus University, Aarhus, Denmark, ⁷CLIMATE Aarhus University Interdisciplinary Centre for Climate Change, Aarhus University, Aarhus, Denmark

Abstract The Northeast Greenland shelf is a broad Arctic shelf located between Greenland and Fram Strait. It is the principal gateway for sea ice export and sea ice-associated freshwater from the Arctic Ocean. Sea ice thickness has decreased by 15% per decade since the early 1990s and meteoric freshwater discharge has increased. The consequence of changing sea-ice and freshwater conditions in the region on ocean dynamics and the biological system remains unknown. Determining the source(s) of freshwater is important to be able to understand how the area will react to future upstream change. Here we present a synoptic survey of the Northeast Greenland shelf and slope with observations of hydrography, the nutrients nitrate, phosphate and silicate, and conservative tracers $\delta^{18}\text{O}$, $\delta^2\text{H}$, and total alkalinity during late summer 2017. We compare these to previously published values, including those which identify Pacific and Atlantic water, the Siberian shelf seas, and the six largest Arctic rivers. We show that a major source of freshwater on the Northeast Greenland shelf during late summer 2017 is the Laptev Sea and find no conclusive evidence of Pacific Water. Our observations indicate a direct link between Northeast Greenland hydrology and processes occurring on Eurasian shelves.

Plain Language Summary The Northeast Greenland shelf is a shallow marine environment between Greenland and the adjacent Fram Strait, where a large fraction of the Arctic Ocean freshwater is exported into the North Atlantic. To predict the regional response to climate change, it is important to determine what the remote sources of freshwater on the shelf are and how these influence mixing. We compare the chemistry of the water found at different locations on the shelf with those found in other areas of the Arctic Ocean to determine where it comes from and conclude that most of the water on the Northeast Greenland shelf in late summer of 2017 is from the Laptev Sea, while surface waters have subsequently been modified by sea ice melt.

1. Introduction

The Northeast Greenland shelf is a broad Arctic continental shelf located between Greenland and the adjacent Fram Strait. Fram Strait is the main conduit for the flux of warm high-salinity Atlantic water northward and the southward flow of cold, low-salinity water exiting the Arctic Ocean. The waters leaving the Arctic Ocean have different formation regions, pathways and modification histories and form density stratified layers in the water column. A significant fraction of the surface water has a meteoric freshwater source and can be advected onto the Northeast Greenland shelf and subjected to additional modification. Changes in upstream conditions therefore may exert significant influence on regional hydrography and biogeochemistry. Gaining an understanding of the sources of water found on the shelf will benefit our ability to predict the response of this environment to any changes taking place upstream in the Arctic Ocean.

Although the determination of freshwater fractions has been performed several times in Fram Strait and further south on the East Greenland shelf (Dodd et al., 2012; Falck, 2001; Sutherland et al., 2009) upstream freshwater source regions have yet to be identified. Although riverine biogeochemical tracer values have been published

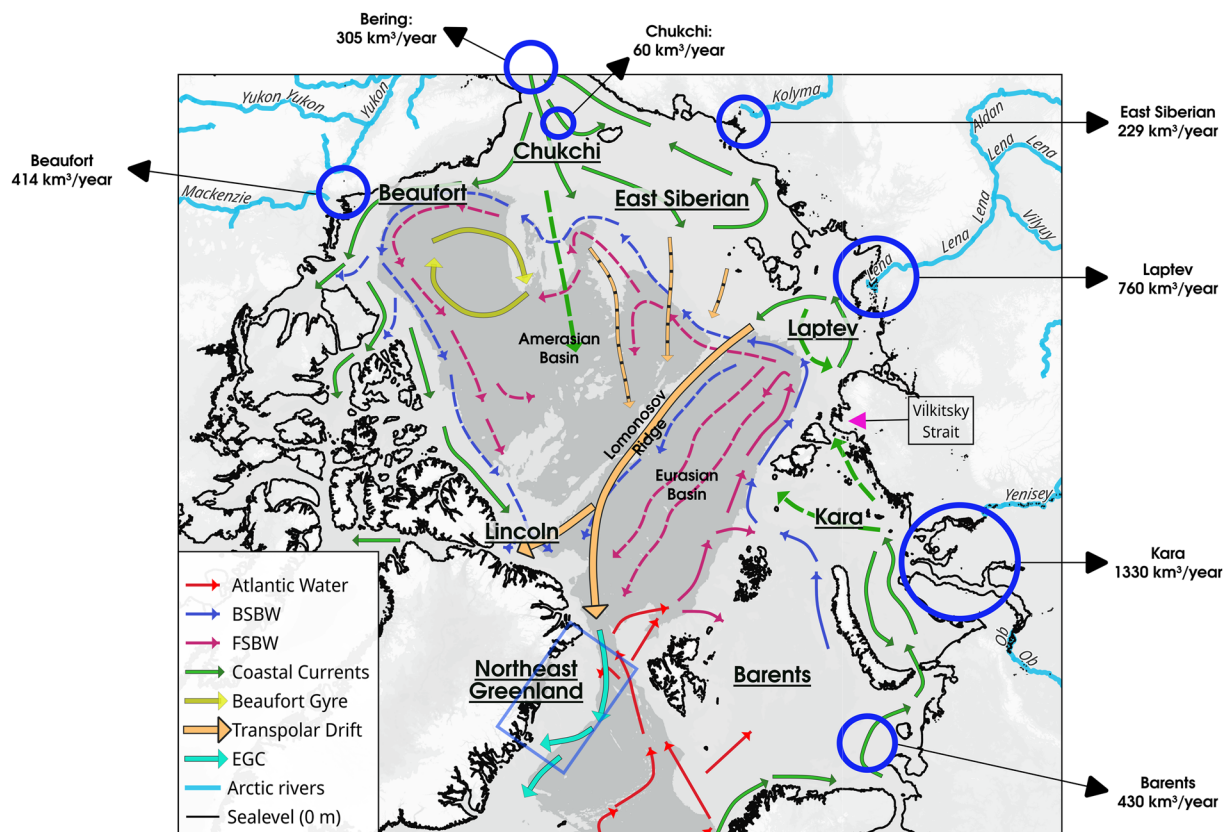


Figure 1. Map of the Arctic Ocean and its major surface and boundary currents based on maps in Rudels et al. (2004) and Aksenov et al. (2016). River GIS shapefile was obtained from <http://arcticgreatrivers.org>. Discharge values are given in the large blue circles as discharge received per shelf sea per annum using values from Shiklomanov et al. (2021). Acronyms FSBW and BSBW are the Fram Strait and Barents Sea branch waters, respectively, and EGC is the East Greenland Current. The Atlantic inflow west of Svalbard is the West Spitsbergen Current. Dashed lines are used where the flow is temporally variable or less information about current specifics is available. The blue rectangle around the Northeast Greenland shelf indicates the study area which is the focus of this paper.

(Cooper et al., 2008), the required number of biogeochemical measurements for the identification of individual rivers are frequently not measured from corresponding downstream oceanographic water samples.

This study aims to remedy this by presenting a cohesive analysis of the Northeast Greenland shelf based on a suite of hydrographical and biogeochemical measurements to determine the synoptic hydrography on the shelf and the dominant source region of the meteoric freshwater found on the Northeast Greenland shelf during late summer 2017.

1.1. Arctic Ocean Circulation

The Fram Strait receives all the water exiting the Arctic Ocean (Figure 1) that is not exported through The Canadian Arctic (or evaporated). As a result, waters with very different spatial and temporal histories are superimposed onto one another as they are geographically constrained in Fram Strait, leading to high hydrographic complexity.

The Atlantic Ocean is the sole deep water conduit to the Arctic Ocean. Even Pacific Ocean input is constrained by the Bering Shelf which has depths shallower than 100 m (Jakobsson et al., 2020) and is considered a source of upper layer water only.

The warm Atlantic current follows two separate pathways into the Arctic. One across the Barents Sea, and the other through eastern Fram Strait which curves eastward north of Svalbard near Yermak Plateau. Both regions form their own halocline water with a slightly different density, as a result of differences in their Atlantic Water temperature (Rudels et al., 2004). North of Svalbard, warm surface water melts sea ice, forming a surface layer. This fresh and cold water inhibits full depth convection during winter and initiates the halocline formation process, which is repeated in subsequent years, creating the Fram Strait Branch Water (FSBW). The Barents

Sea forms its own halocline water. This has a sea ice melt component but also has additional freshwater sources, including but not limited to the Norwegian Coastal Current and freshwater from rivers discharging into the Kara Sea, each of which contribute to limiting the depth of winter convection and the formation of the Barents Sea Branch Water (BSBW). The Nansen Basin is dominated by FSBW while the Amundsen Basin contains a mixture of both branches with BSBW the dominant branch (Figure 1) (Rudels, 2021; Schauer et al., 2002).

As Atlantic water is transported around the Arctic Ocean, freshwater is added incrementally by Arctic rivers discharging onto the continental shelves, sea ice melt, and precipitation (Haine et al., 2015). Following Atlantic water in a counter clockwise direction, Barents Sea freshwater is dominated by precipitation and by subpolar coastal freshwater of the Norwegian Coastal Current (Rudels, 2021). This is followed by input from the rivers Ob' and Yenisey which discharge directly into the Kara Sea. Observations of the Ob'-Yenisey plume show that freshwater transport from the Kara to the Laptev Sea through Vilkitsky Strait depends on the persistence of along-shore south-westerly winds and in their absence the water is exported off-shelf (Osadchiev et al., 2020). The Lena river plume direction also depends on atmospheric forcing, with off-shelf transport occurring when winds force anticyclonic circulation which transports freshwater across the shelf and into the Arctic Ocean where, together with underlying Atlantic water, it is entrained in the Transpolar drift (Bauch et al., 2009). Biogeochemical and hydrographic surveys of the Transpolar drift regions show both riverine influence (Charette et al., 2020; Paffrath et al., 2021) and the lower halocline (Kikuchi et al., 2004; Rabe et al., 2022). The remaining Lena River water is transported by a narrow coastal current to the East Siberian Sea.

The East Siberian Sea shelf receives additional river discharge from the Kolyma river and is advected toward the Chukchi Sea (Osadchiev et al., 2020). The water entering the Arctic from the Pacific Ocean through the Bering Strait and onto the Chukchi shelf is also considered a freshwater source containing a large fraction of meteoric water, including the runoff from the Yukon River. Much of this water is captured by the Beaufort Gyre, as is a portion of the Mackenzie River water on the Beaufort Sea shelf. A small portion of the Pacific Water inflow is captured by a counter current across the East Siberian Sea and potentially entrained into the Transpolar drift, subsequently exiting in Fram Strait. Water transported via this route has an upper halocline with salinities between 33.1 and 34.2, formed by brine rejection during sea ice formation on the continental shelf, which is characterized by high nutrient concentrations due to processes taking place in the Chukchi and East Siberian Seas (Alkire et al., 2021; Anderson et al., 2013; Jones & Anderson, 1986).

Fram Strait is the ultimate destination for all the Arctic freshwater that is not exported through the Canadian Archipelago. This means that water masses from all these sources with vastly different histories are superimposed here based on their density.

Only water relatively close to the surface compared to the full depth of Fram Strait can be advected onto the Northeast Greenland shelf due to bathymetric constraints. This limits the available water types to those found at depths less than the maximum trough depth at the shelf edge (300–370 m) plus any deeper water available for entrainment during upwelling events (Arndt et al., 2015). The top few hundred meters include most of the typically Arctic-associated hydrographic features, such as the summer mixed layer, and the cold halocline layer with temperatures close to freezing and salinities between the Lower Halocline Water (LHW) at $S \sim 34.2$ (Jones et al., 1991) and those of the (summer or winter) mixed layer. Subsurface Atlantic water can take one of several routes across the Arctic. Canadian Basin Atlantic Water (CBAW) has circulated across the Canadian Basin and is cooler, compared to Eurasian Basin Atlantic Water (EBAW) which has circulated only in the Eurasian Basin (Figure 1). Together, the EBAW and CBAW are sometimes referred to as Arctic Atlantic Water when they exit the Arctic Ocean at Fram Strait. The final source of Atlantic water that may be transported onto the Northeast Greenland shelf is Return Atlantic Water (RAW). This is Atlantic Water from the northward inflow current west of Svalbard and is the warmest found on the shelf (Figure 2). The local freshwater contributions from Nioghalvfjærdsbrae (79°N) and Zachariae Isstrøm are small compared to those from the Arctic great rivers (Haine et al., 2015) and mix to such an extent to not be distinguishable proximal to the shelf break (Huhn et al., 2021).

The precise residence time of waters on the Northeast Greenland Shelf itself is currently unknown. Although Atlantic Water flow rates are available, they rely on the accurate estimation of the Pacific water fraction (Lin et al., 2022), which may be biased through denitrification in the Laptev Sea (Bauch et al., 2011; Nitishinsky et al., 2007; Sun et al., 2021). The transport of the off-shelf East Greenland Current has been estimated at ~ 3 Sv, and to be barotropically driven and contain superimposed eddies with widths around 10 km and depths to 400 m (Foldvik et al., 1988).

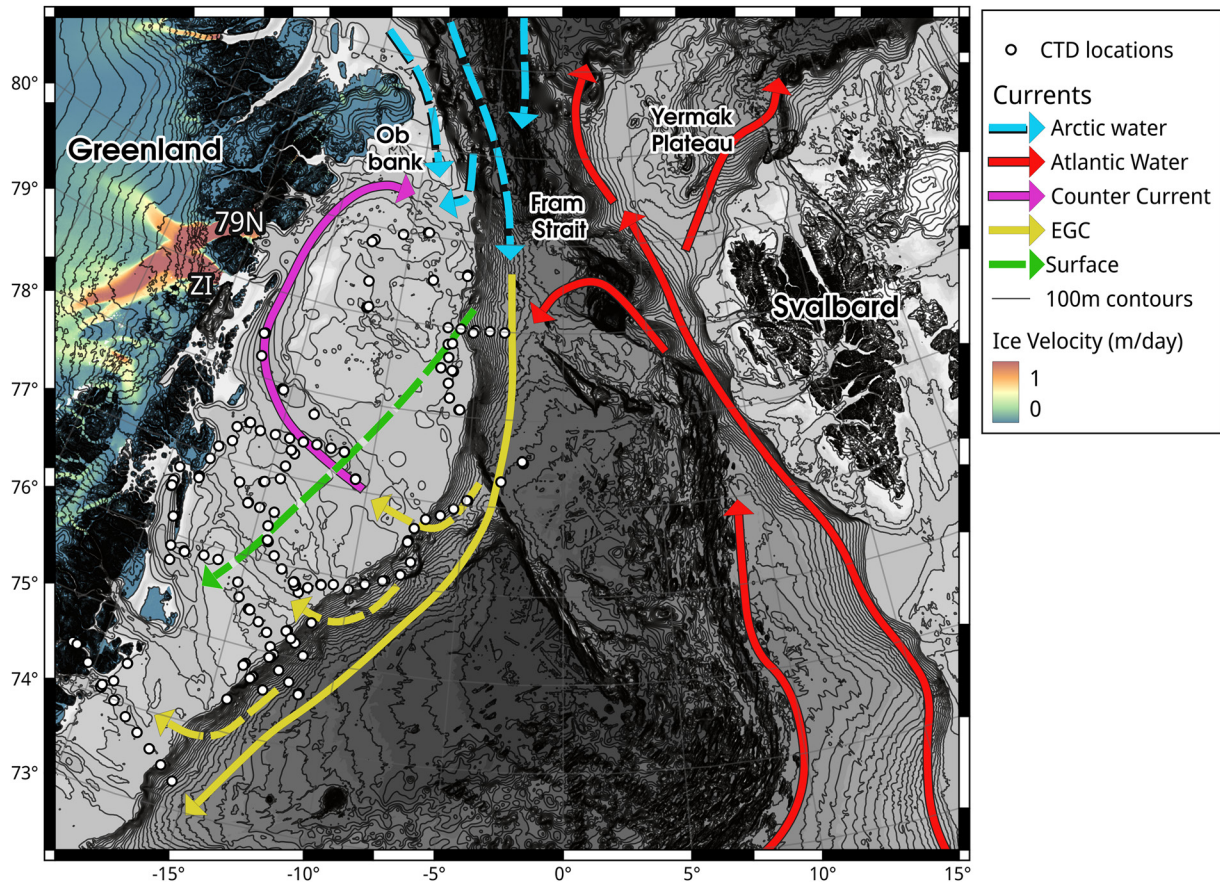


Figure 2. Map with the Conductivity Temperature Depth stations that were part of this study and the major known (solid) and hypothesized (dashed) currents. Surface water that is part of the off-shelf currents (including Arctic Water, the East Greenland Current or EGC, and the Atlantic Water) is available for transport onto the Northeast Greenland shelf. On the shelf, the Northeast Greenland Counter Current is relatively well established in literature. Less is known about the cross-shelf surface water. Return Atlantic Water is entrained into the EGC and is known to be available inside Belgica trough, where the counter current is initiated. It is possible that other troughs are also conduits for Atlantic Water though this depends on sill depths. Two outlet glaciers of the Northeast Greenland Ice sheet, Niogerhalfjersbrae (79°N) and Zachariae Isstrom (ZI) are identified by their ice velocity.

A subsurface water type referred to as East Greenland Shelf Water by Budéus and Schneider (1995) and as Polynya Intermediate Water by Bignami and Hopkins (1997) was previously identified on the Northeast Greenland shelf. These authors argued for its local formation in the Northeast Water polynya due to its geographical proximity to this feature. This polynya was an open water feature in summer and is thought to contain thinner ice than is expected from atmospheric conditions in winter (Smith IV & Morison, 1998; Smith & Barber, 2007). It used to be established just northeast of the Norske Øer ice barrier and south of the Ob Bank ice barrier, where large icebergs would run aground and restrict the advection of ice into the region, while ice was simultaneously being removed by the anticyclonic surface Northeast Greenland Counter Current (Figure 2). The Norske Øer ice barrier has since ceased to be a persistent feature in the region (Sneed & Hamilton, 2016) and is unlikely to play as large a role now. Neither the Norske Øer nor the Ob bank ice barrier were present in the late summer of 2017.

2. Tracking Freshwater Source Through Tracers

Source regions of freshwater with different characteristics may be identified using tracers. These are (quasi-) conservative chemical signatures with a known concentration at each source and known to respond primarily to physical mixing processes. They have been used extensively to determine freshwater fractions, specifically meteoric water (precipitation and river discharge), sea ice melt, and Pacific Water fractions (Bauch et al., 2011; Dodd et al., 2012; Falck, 2001; Falck et al., 2005; Sutherland et al., 2009).

The methodology for using tracers to determine the origin of different freshwater fractions relies on knowing accurate and distinguishable tracer concentrations for each end-member and inserting them into a system of linear

equations (Jones et al., 2008). Common tracers in an Arctic Ocean three end-member system to identify fractions of sea ice melt, meteoric water, and Atlantic Water are stable oxygen isotopic composition ($\delta^{18}\text{O}$) and total alkalinity (TA). These have end-members which are distinguishable from one another and respond to freezing in a predictable way (O'Neil, 1968; Rysgaard et al., 2007).

The most common tracer for identifying Pacific water, which enters the Arctic Ocean through Bering Strait, is the N:P ratio. Although its constituents are not conservative, their ratio is considered quasi-conservative and can be calculated using either the ratio of total dissolved inorganic nitrogen (Yamamoto-Kawai et al., 2008) or that of dissolved nitrate (Falck, 2001; Falck et al., 2005; Jones et al., 1998) to dissolved phosphate concentration. Water transported into the Arctic via the Bering Strait has a lower nitrogen concentration relative to phosphate compared to Atlantic-sourced water. This difference is further enhanced during advection across Chukchi Sea shelf sediments, where bacterial denitrification takes place (Codispoti et al., 1991; Cooper et al., 1999; Tanaka et al., 2004). More recently denitrification has also been found to occur in Laptev shelf sediments (Bauch et al., 2011; Nitishinsky et al., 2007; Sun et al., 2021) close to the source of the Transpolar drift which could bias fraction attribution to Pacific Water. The Upper Halocline Water (UHW) at its salinity range between 32 and 34, and high nutrient concentrations is also associated with Pacific water inflow (Anderson et al., 2013; Nguyen et al., 2012).

3. Materials and Methods

Sampling for the present study was done on from two 3-week cruises with RV Dana to NE Greenland during August–September 2017. Leg 1 was carried out in the context of a monitoring project by the Government of Greenland and Leg 2 as a research expedition (NorthGreen2017) organized by the Department of Geoscience and the Arctic Research Center, Aarhus University. The combination of the two cruise legs, made it possible to save significant transit time for both expeditions and low sea-ice cover made it possible to work in a larger area on the Greenland shelf than expected, up to 80°N (Figure 2).

In total 115 Conductivity Temperature Depth (CTD) stations were sampled. We used a rosette (12 Niskin bottles) to collect water at 1 m, 5 m, 10 m, 20 m, deep chlorophyll maximum, 30 m, 50 m, 100 m, 200 m, 400 m, and the bottom. A CTD (Seabird 911 system) attached to the rosette measured conductivity, temperature, and pressure. Two oxygen sensors were also mounted on the rosette. The CTD sensors were calibrated yearly by the manufacturer and uncertainty of salinity was typically within the range 0.005–0.010. We use the term salinity (S) for practical salinity (psu, practical salinity scale 1978), the term temperature (T) refers to the potential temperature (Θ). The terms depth and pressure are also considered interchangeable.

At every station, we collected water for TA analysis at all depths in 13 mL glass vials to which we added 50 μL of HgCl_2 (5% solution); 11 water bottles (50 mL in polyethylene vials) for nutrients analyses at all depths and frozen for later analysis (silicate, nitrate + nitrite, and phosphorous); 11 water (glass vials of 2 mL) for water isotope analysis ($\delta^{18}\text{O}$; $\delta^2\text{H}$). Small drifting sea ice pieces were collected with a net from the deck of RV Dana for similar analysis.

Samples for TA were stored at 4°C until analysis. Samples for nutrient analysis were frozen in polyethylene vials until later analysis. The vials were rinsed several times with water from the specific depth before filling and freezing. TA was determined by Gran titration (Gran, 1952) using a TIM 840 titration system (Radiometer Analytical, ATS Scientific), consisting of a Ross sure-flow combination pH glass electrode (Orion 8172BNWP, Thermo Scientific) and a temperature probe (Radiometer Analytical). A 12 mL sample was titrated with a standard 0.05 M HCl solution (Alfa Aesar). Routine analysis of Certified Reference Materials (provided by A. G. Dickson, Scripps Institution of Oceanography; <http://andrew.ucsd.edu/co2qc/>) verified that the accuracy of TA was $\pm 3 \mu\text{mol kg}^{-1}$. The isotopic compositions ($\delta^{18}\text{O}$; $\delta^2\text{H}$) of the samples were analyzed with a Cavity Ringdown Spectrometer, L2130-i Isotopic H2O (Picarro Inc., USA). Nine injections were taken from each sample and vapourized and the first three were excluded to remove any residual results from the previous sample. Vapor content, $\delta^2\text{H}$ and $\delta^{18}\text{O}$ values were calculated relative to certified standards. Four standards were measured at the beginning and end of the sample set. The external standards used to calibrate the results were Vienna Standard Ocean Water 2 ($\delta^2\text{HVSMOW}$, $\delta^{18}\text{OVSMOW}$) (VSMOW2), Greenland Ice Sheet Precipitation ($\delta^2\text{HGISP}$, $\delta^{18}\text{OGISP}$) (GISP), and Standard Light Antarctic Precipitation 2 ($\delta^2\text{HSLAP2}$, $\delta^{18}\text{OSLAP2}$) (SLAP2). Detection limit for nutrient concentrations were 0.1 $\mu\text{mol kg}^{-1}$ (NO_3^-), 0.06 $\mu\text{mol kg}^{-1}$ (PO_4^{3-}), and 0.2 $\mu\text{mol kg}^{-1}$ (Si).

Table 1
Datasets and Relationships Used for Comparison With 2017 Northeast Greenland Shelf Data to Determine Possible Source Location(s) for Water Found on the Northeast Greenland Shelf

Tracer relationship	Region	Detail used	Paper
NO ₃ ⁻ :PO ₄ ³⁻	Laptev	Supplementary data	Supplement to Thibodeau et al., 2017
	East Siberian Sea	Surface water average	Table 1 in Semiletov, 2005
	Atlantic & Pacific	Linear fit	Figure 2 in Jones et al., 1998
TA:S	Atlantic & Pacific	End member values	Table 2 in Sutherland et al., 2009
	Major rivers	End-member values	Table 1 in Cooper et al., 2008
δ ¹⁸ O:S	Arctic Deltas	Polynomial fit	Figure 2 in Namyatov, 2021
δ ² H:δ ¹⁸ O	Major rivers	Linear fit lines	Table 1 in Yi et al., 2012
	Global Meteoric Water Line	Linear fit line	Craig, 1961
	Arctic Meteoric Water Line	Linear fit line	Equation 3 in Mellat et al., 2021
Si:AOU & PO ₄ ³⁻ :AOU	Laptev Sea water column	Linear fit lines	Figure 4 in Sun et al., 2021
Sea ice melt	Local	Own measurements (5)	TA: 393, 130, 364, 61, 70
			δ ¹⁸ O: -3.02, -2.95, -1.52, -1.56, -2.67

Data from the CTD casts from both cruises were combined into a 1 m (± 0.5) binned dataset. A second dataset was created by combining the CTD bottle data with the analyses of $\delta^{18}\text{O}$, $\delta^2\text{H}$, TA, and nutrients based on cruise, station, and depth. The freezing line, oxygen saturation w.r.t. the atmosphere, and apparent oxygen utilisation (oxygen loss attributed to photosynthetic use, $\text{AOU} = [\text{O}_2]_{\text{s,t,p}} - [\text{O}_2]_{\text{obs}}$) were calculated with the Julia programming language (Bezanson et al., 2017) implementation of the TEOS-10 (Feistel, 2012) library.

To identify potential freshwater source locations, we compared our data to literature (Table 1). All maps were produced in QGIS (QGIS Development Team, 2022) with bathymetric data from IBCAO v4 (Jakobsson et al., 2020) and ice velocity from QGreenland (Moon et al., 2020).

4. Results and Interpretation

First, we manually assigned each individual CTD cast to one of five groups based on their clearly distinguishable shape in a *TS* diagram (Figure 3) and according to the presence of specific water types (Table 2). This was done first to avoid biasing our interpretation by taking geography as a starting point. Average profiles for each group are shown in Figure 4 together with the Brunt Väisälä frequency square (N^2) and the oxygen saturation w.r.t. that of the atmosphere. Mapping their longitude and latitude did show a geographical relationship with CTD cast group (Figure 5).

4.1. Geographical Groups

4.1.1. North Shelf Group

The North Shelf group stations (Figures 3a, 4a–4d, and 5) are found in the area formerly associated with the Northeast Water Polynya. This group has a summer halocline identifiable from temperature and salinity (Figures 4a and 4b) with a Brunt-Väisälä frequency squared maximum (N^2 , Figure 4c) at around 10 m depth. Below the summer halocline there is a relatively more homogeneous layer down to a depth of 50 m which is associated with the Northeast Greenland Winter Water (NGWW). This is interpreted as the remnant of the winter mixed layer. In the upper part, between 20 and 30 m a dissolved oxygen maximum occurs which reaches almost 100% of atmospheric saturation (Figure 4d). This group is marked by the absence of AW, RAW, and LHW (Figure 3a), rather showing direct diapycnal mixing between EBAW to the freezing line with which it intersects at a salinity of ~ 32.5 and at a depth of ~ 80 m (Figure 4b).

4.1.2. Main Shelf Group

Stations in the main shelf group (Figures 3b, 4a–4d, and 5) show both a subsurface halocline and remnant winter mixed layer with an oxygen maximum depth similar to the North shelf group (Figures 4a–4e). This group is both

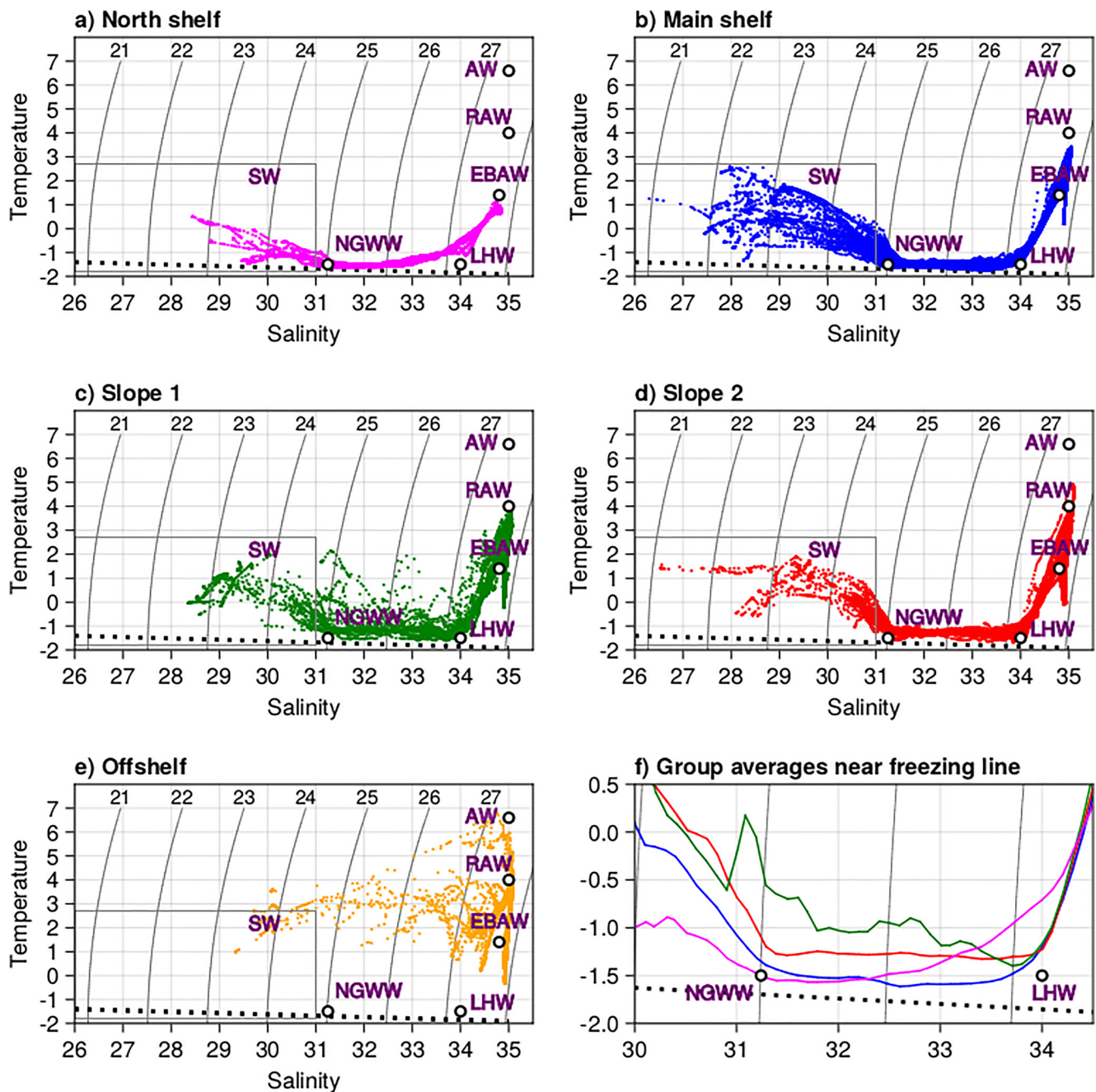


Figure 3. Hydrography on the Northeast Greenland shelf from Conductivity Temperature Depth casts. These are the five (a–e) groups which were identified by their shape in the TS diagram per the water types that were present (Table 2). Their names were subsequently chosen after they were mapped (Figure 5). (f) Closeup of the cold halocline layer where present, for example, all groups except the Offshelf group.

fresher and warmer than the North shelf group at densities $\sigma_T < 25$ above the NGWW. This group contains both LHW and NGWW and the TS data connecting these two water masses follows the freezing point line closely, indicating a well-established cold halocline layer (Figure 3b). This is the dominant group in and south of Belgica Trough away from the slope (Figure 5).

4.1.3. Slope 1 Group

The stations selected to be part of this group (Figures 3c, 4e–4h, and 5) were those which deviated greatly from the freezing line at salinities associated with the cold halocline layer (Figure 3c). This is interpreted as evidence of

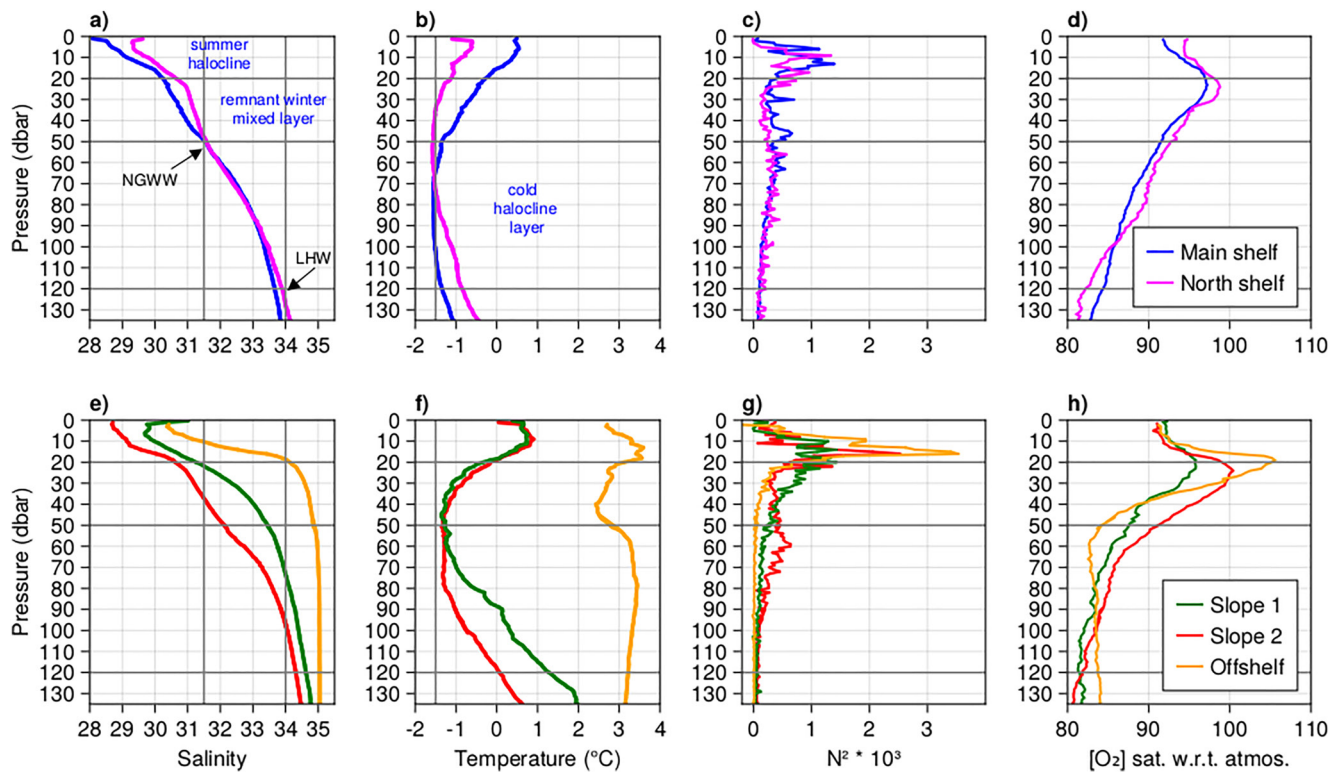


Figure 4. Profiles of Conductivity Temperature Depth cast (a and e), Salinity (b and f), potential temperature (c and g), and Brunt–Väisälä frequency squared (d and h). Dissolved oxygen saturation with respect to the atmosphere for shelf groups (top) and slope and off-shelf groups (bottom). The depth maxima for $N^2 \times 10^3$ and $[O_2]_{\text{sat}}$ for each group respectively are North shelf (9 m 1.1, 24 m 99%), Main shelf (13 m 1.4, 23 m 97%), Slope 1 (14 m 1.43, 22 m 96%), Slope 2 (16 m 2.5, 24 m 100%), and Offshelf (16 m 3.5, 19 m 106%).

mixing with the warmer Offshelf group. This group contains all defined water types except for AW but it lacks a remnant of the winter mixed layer which differentiates it from North and Main shelf, and Slope 2 groups. Instead, it has a summer halocline which is deeper than that of any other group. The dissolved oxygen saturation relative to the atmosphere is lowest compared to that of the other groups although it is present at the same depths.

4.1.4. Slope 2 Group

The profiles in this group (Figures 3c, 4e–4h, and 5) are similar to the Main shelf group profiles, their main difference being that the Slope 2 *TS* plot (Figure 3c) does not follow the freezing line as closely, being around 0.5°C warmer than main shelf stations on average (Figure 3f). This group does have a remnant winter mixed layer, but it is less homogeneous or well-defined than that of the shelf groups, being both deeper and across a larger salinity range.

4.1.5. Offshelf Group

The Offshelf group (Figures 3–5) is the only group entirely lacking a cold halocline layer that is, the layer between the NGWW and the LHW which follows the freezing point line. Mixing occurs directly between the Atlantic source water (AW, RAW, EBAW) and SW. Average profiles (Figures 4e–4h) for this group show a summer halocline with a maximum N^2 at 16 m. The difference in depth between the maximum N^2 and the maximum oxygen saturation is only 3 m for this group, the smallest of all groups and it is the only group with a supersaturation in dissolved oxygen with respect to the atmosphere. Cooling of up to 1°C occurs between 20 and 50 m (Figure 4f). At depths below 50 m temperatures remain just over 3°C while the salinity remains at 35.

4.2. Freshwater Sources

To determine the difference between meteoric and sea ice melt freshwater sources, an assessment was made of the TA and stable water oxygen isotopic ($\delta^{18}O$) composition variation with salinity (Figures 6a and 6b). The sea

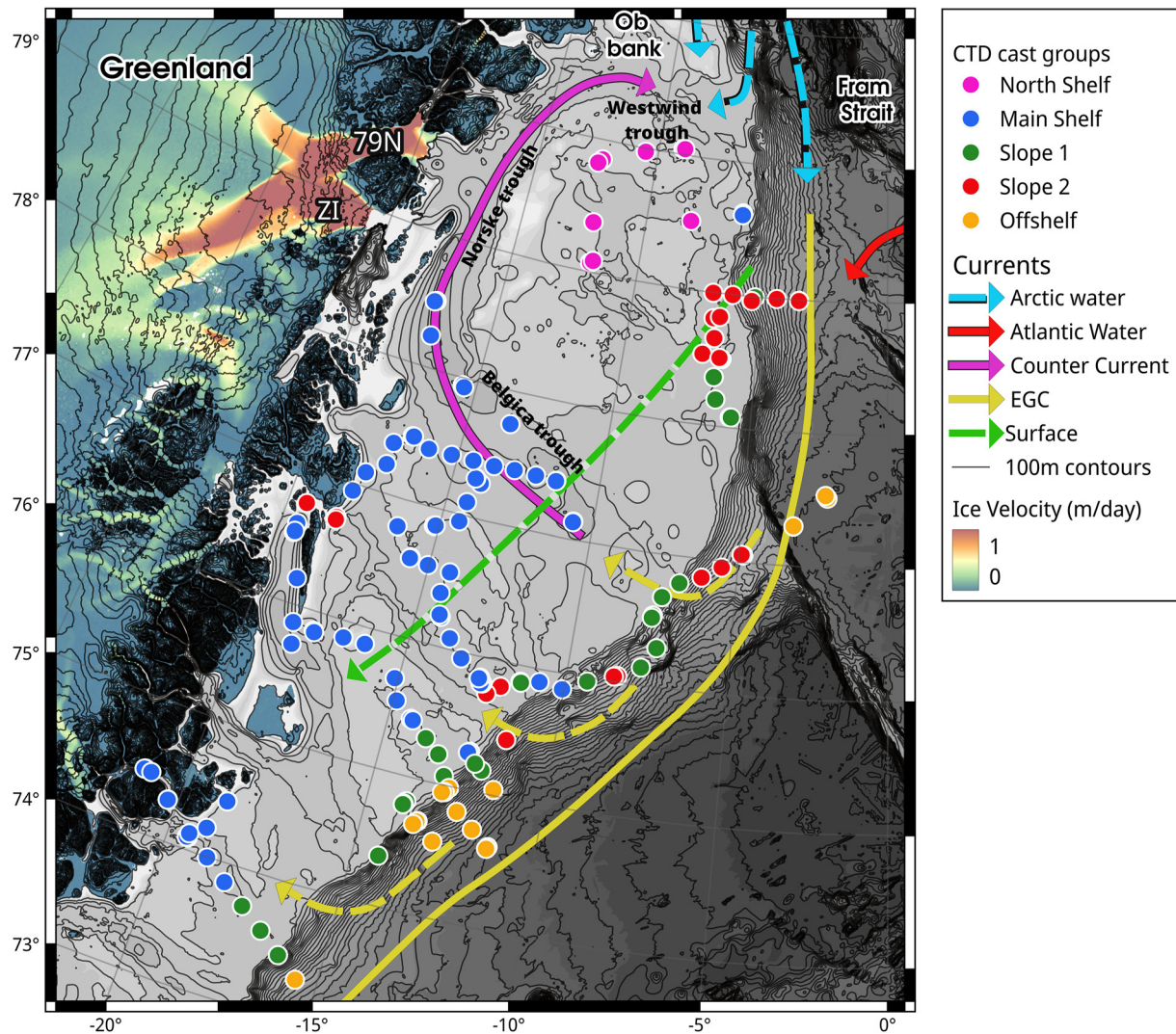


Figure 5. Conductivity Temperature Depth group locations plotted in their geographical setting with known and hypothesized currents (currents as described in Figure 2). Solid currents are those which have been described in the literature, and dashed currents are hypothesized.

ice melt water lines were obtained from local measurements (Table 2). The data is characterized in both plots by two slopes which diverge at a salinity of 31.4, that is, the NGWW. This salinity is also associated with the highest dissolved oxygen saturation with respect to the atmosphere. The presence of this divergence for both tracers in the direction of the sea ice melt end-member indicates a clear increasing sea ice melt influence with decreasing salinity above the NGWW.

In the cold halocline layer between NGWW and LHW, $\delta^{18}\text{O-S}$ values are found at higher salinities than the regression lines obtained from Cooper et al. (2008) and Namyatov (2021) (Figure 6b). This is interpreted as the influence of brine on river discharge modified Atlantic water (Bauch et al., 2011). Distinguishing between different riverine or shelf sources is difficult using these tracers since each of the lines are increasingly close together as they approach the Atlantic water end-member. Although these may be good tracers at lower salinities, closer to their discharge source, they are inappropriate for identifying remote source water on the Northeast Greenland shelf, especially where additional deviation from the mixing line is introduced by brine drainage and sea ice melt. The same is true for the Pacific water end-member, which clearly falls close to several of the mixing lines.

To distinguish between Pacific and Atlantic source water, we assessed the nitrate to phosphate ratio (N:P, Figure 7a) and the presence of UHW (Figures 7b and 7c). The N:P for our data follows the Atlantic water regression line (Jones et al., 1998) down to $\sim 6 \mu\text{mol/kg}$ nitrate. At nitrate concentrations below this, the corresponding

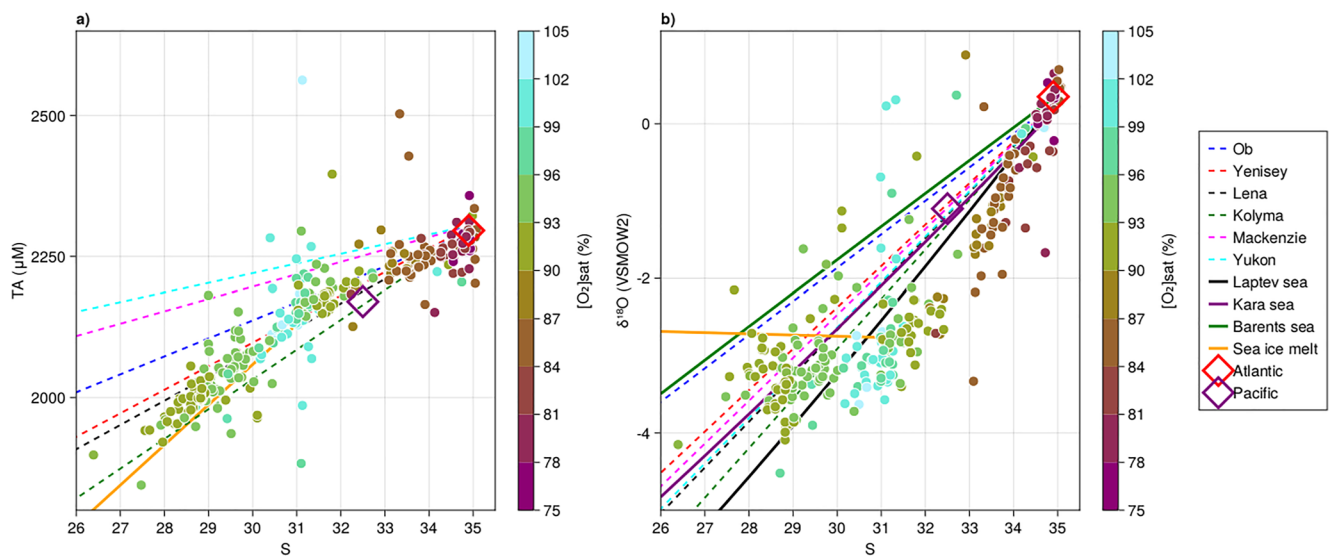


Figure 6. Conductivity Temperature Depth bottle data for all depths and geochemical tracers. (a) Total alkalinity (TA) with best fit line sources shown in Table 2: For individual rivers from Cooper et al. (2008) and Atlantic and Pacific end members from Sutherland et al. (2009). (b) $\delta^{18}\text{O}$ plotted against practical salinity with Eurasian shelf polynomials from Namyatov (2021) and river lines from Yi et al. (2012). Sea ice melt lines were calculated using the average of our measurements (Table 2) against a nominal salinity of 4 which was not measured. Note that this is a high salinity value for multiyear ice.

phosphate concentrations are relatively constant at around $0.5 \mu\text{mol/kg}$, a signal commonly associated with a denitrification signal. This is generally interpreted as denitrification from Pacific water crossing the Chukchi shelf. This interpretation is likely erroneous for our dataset since it compares well to data from the Laptev Sea which expresses a similar pattern (Thibodeau et al., 2017) even though this region does not contain Pacific water. Values of nitrate versus phosphate observed in the eastern versus western East Siberian Sea (Semiletov, 2005) also indicate that Pacific water may not necessarily have the highest influence on this signal in the Siberian Arctic shelf areas. At the lowest and most sea ice melt influenced layers the nitrate is almost entirely depleted with a median dissolved nitrate concentration of $0.0 \mu\text{mol/kg}$ which limits the usability of this quasi-conservative tracer. Phosphate concentrations are not similarly depleted.

The UHW (Figures 7b and 7c) is generally associated with a sharp increase in nutrient concentrations, low oxygen concentrations and is present in the Canadian Basin at salinities between 32 and 34 (Anderson et al., 2013; Nguyen et al., 2012). We see no sharp increase in nutrient concentrations at these salinities. We interpret this as the absence of UHW on the Northeast Greenland shelf in late summer 2017.

Values for hydrogen and oxygen stable water isotopes ($\delta^2\text{H}:\delta^{18}\text{O}$) fall between the Arctic Meteoric Water Line (Mellat et al., 2021) and the best fit line for the Lena River (Yi et al., 2012). The AMWL was calculated using terrestrial summer measurements across the Arctic and so does not provide a single source location, rather it is taken as an average across the entire Arctic. Contrary to these, Yi et al. (2012) created flux weighted average

Table 2
Water Types and Conductivity Temperature Depth Group Assignment

	Properties		Group characteristics				
	S	θ ($^{\circ}\text{C}$)	Offshelf	Main shelf	North shelf	Slope 1	Slope 2
Atlantic Water (AW)	35	6.6	X				
Return Atlantic Water (RAW)	35	4.0	X	X		X	X
Eurasian Basin Atlantic Water (EBAW)	34.8	1.4	X	X	X	X	X
Lower Halocline Water (LHW)	34.0	-1.5		X		X	X
Northeast Greenland Winter Water (NGWW)	31.4	-1.5		X	X		X
Surface Water (SW)	<31.4	-	X	X	X	X	X

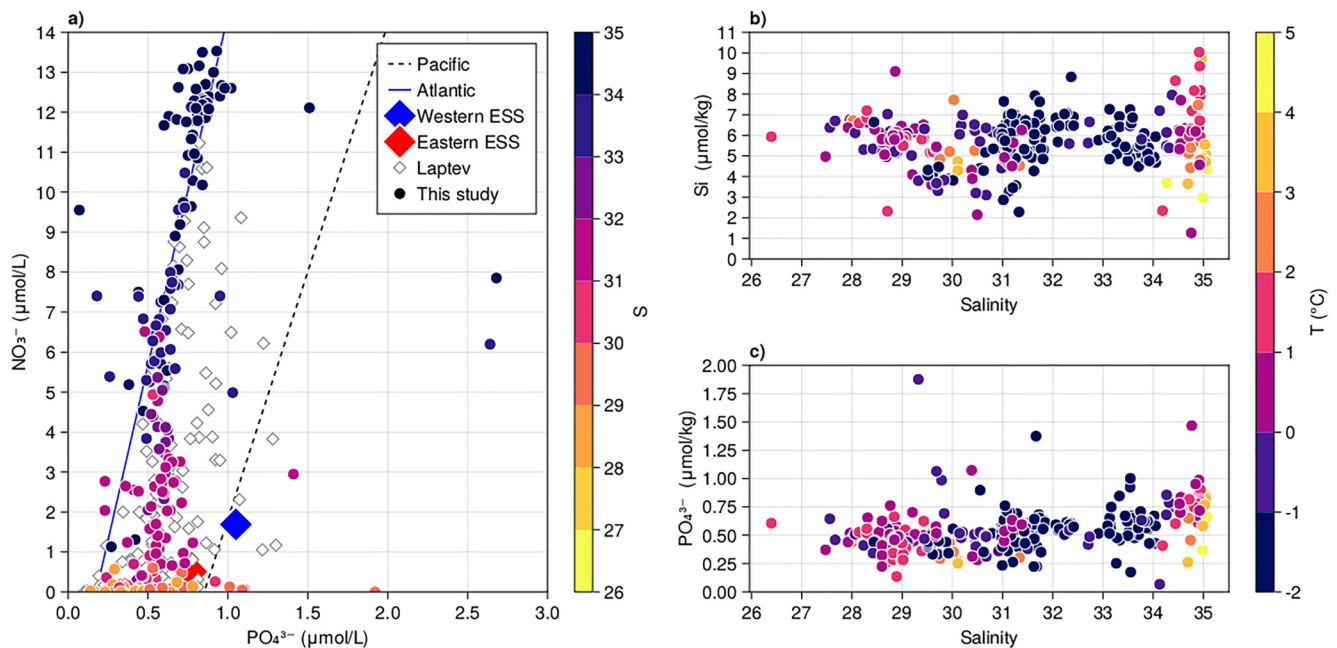


Figure 7. Conductivity Temperature Depth bottle data for all depths and geochemical tracers of (a) N:P superimposed on Laptev Sea data from Thibodeau et al. (2017). Pacific (black dashed) and Atlantic (blue solid) regression lines obtained from Jones et al. (1998). Two nutrients which should indicate Upper Halocline Water (UHW) presence as a dramatic increase in concentration at salinities between 32 and 33 (b) Si:S and (c) PO_4^{3-} :S. Neither of these tracers shows this clear.

regression lines for each of the 6 major Arctic rivers (Figure 8). Due to the proximity of the data to the Lena River line and the distance between the data and any other river we interpret these data as containing a significant volume of Lena River water. At the lowest values of both $\delta^2\text{H}$ and $\delta^{18}\text{O}$ some datapoints approach the GMWL. This may reflect the influence of precipitation. The usability of this tracer for the purpose of identifying individual rivers will require future verification.

Neither silicate nor phosphate are conservative tracers as both are utilized by organisms in the water column. It was therefore surprising to find that when these are plotted against apparent oxygen utilization (Figure 9), the difference between the oxygen solubility and the dissolved oxygen measured, our data follows the relationship found by Sun et al. (2021) for the Laptev Sea closely. This observation might be produced by two processes: The first is repeated production and remineralization cycles occurring in such a way that this relationship is exactly maintained during successive seasonal cycles. The second that there is too little water column biological activity during the time taken for water to be advected across the Arctic Ocean to result in an observable change, and the layer is created and maintained solely by seasonal physical processes. The latter is plausible only if either the sea ice cover is extensive and limits photosynthetically active radiation during water transport across the Arctic Ocean or if the nitrate concentrations are limited to a point where primary production is inhibited.

5. Discussion

The most remarkable hydrographic feature on the Northeast Greenland shelf is the extensive cold halocline layer, which occupies the *TS*-space along the freezing point line (Figures 3 and 4) between the NGWW and the LHW. The presence or absence of these two water types is geographically correlated (Figure 5). This contrasts with the relationship between geochemical tracers and salinity which show a clear change in slope with salinity at the NGWW but has a much smaller or absent signal for the LHW. Our data best support the hypothesis that the layers above the NGWW, for example, the remnant winter mixed layer, summer halocline and surface water are strongly sea ice melt influenced, where the cold halocline layer is both brine and Lena river discharge influenced.

Although the NGWW is the most prominent feature on the shelf and is interpreted as the maximum depth of winter mixing on the Northeast Greenland shelf, not much can be definitively concluded about its formation. Since the residence time of waters on the shelf is currently unknown, it is difficult to determine whether this

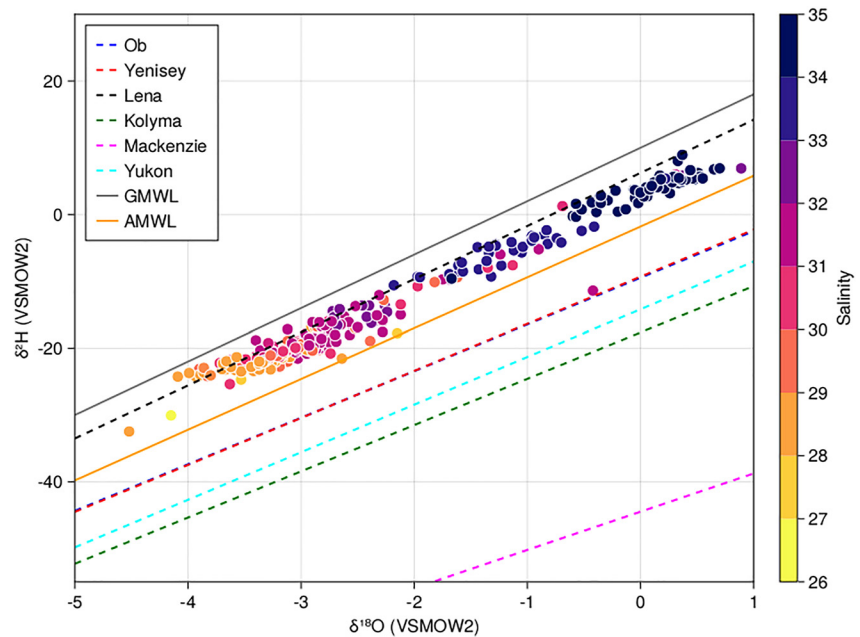


Figure 8. Conductivity Temperature Depth bottle data stable water isotopic ratio of deuterium ($\delta^2\text{H}$) against oxygen ($\delta^{18}\text{O}$) from the Northeast Greenland shelf together with meteoric regression lines for each river from Yi et al. (2012) and global (GMWL, Craig, 1961) and Arctic meteoric water lines (AMWL, Mellat et al., 2021). Note that rivers Yenisey and Ob' are indistinguishable from one another in this figure due to overlap.

water type is solely a product of a local process as suggested in the past (Bignami & Hopkins, 1997; Budéus & Schneider, 1995; Budéus et al., 1997), for example, from multi-annual winter mixing of water trapped in the Northeast Water polynya, or whether it is advected. A significant difference between older studies and ours is that the NGWW is at least 1 salinity unit fresher than it was in the 1990s, while temperatures remain in the same range (our Figures 3 and 4; Bignami & Hopkins, 1997; Figure 2). This implies a large increase in freshwater

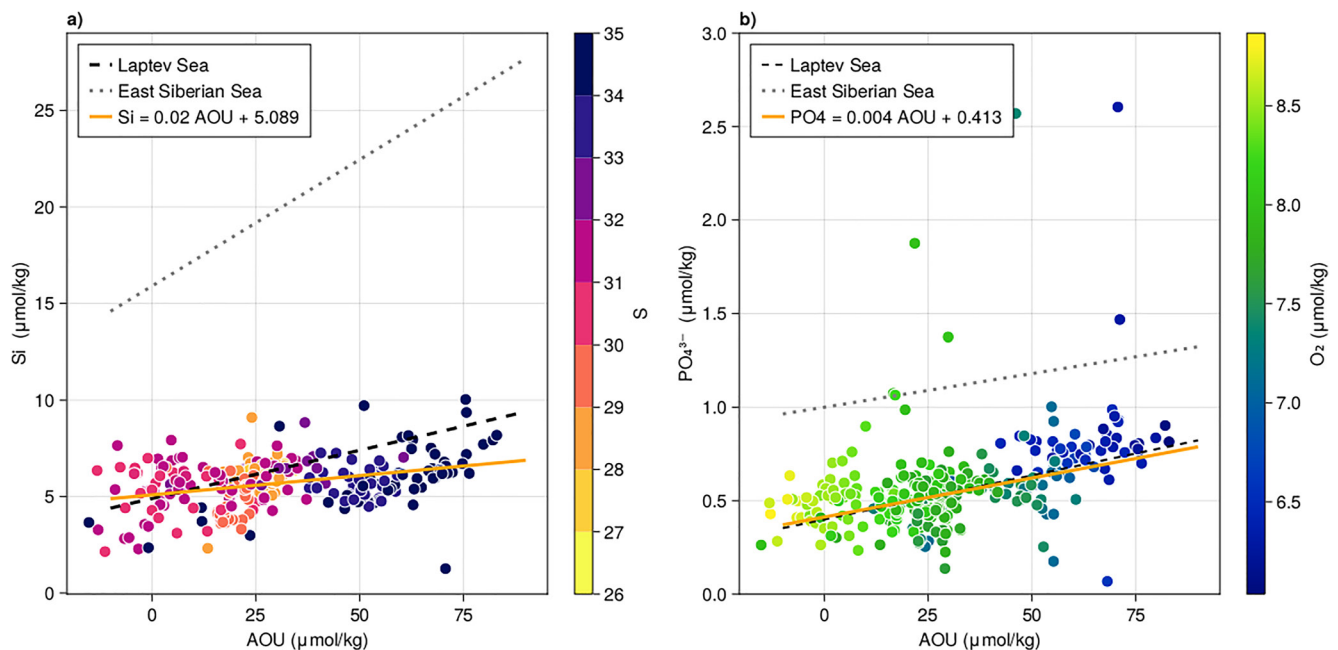


Figure 9. Conductivity Temperature Depth bottle data from this study (points) for all depths of non-conservative nutrient (a: silicate; b: phosphate) to apparent oxygen utilization (AOU) with the regression lines for the Laptev and East Siberian Sea (Sun et al., 2021).

input, which influences the energy requirement for winter mixing to the same depths as during winters with lower volumes of freshwater.

In other parts of the Arctic Ocean, similar remnant winter mixed layers and/or types have been identified such as the Polar Mixed Layer (PML), defined as the depth of the temperature minimum remaining after winter convection in the Canadian Arctic (Peralta-Ferriz & Woodgate, 2015). In the Beaufort Sea, the PML has been identified by its S, TA, and $\delta^{18}\text{O}$ properties (Lansard et al., 2012). There, the PML mixes down to the UHW which is not present in our dataset (Figure 7) although it may be present north of Ob bank where we have no data as was found by Budéus et al. (1997). On the Northeast Greenland shelf, the NGWW mixes with the LHW instead. Similar to findings in the Beaufort Sea, the sharp inflection in the TA:S and $\delta^{18}\text{O}$:S toward the sea ice melt regression line (Figures 6a and 6b) imply that water with densities of $\sigma_T < 25$ and above the NGWW is strongly influenced by sea ice melt, where water found at $\sigma_T > 25$ and below the NGWW, consist primarily of brine-modified river water. This influence by sea ice melt in the surface layer may also be the reason for the dissolved oxygen sub-saturation in the surface mixed layer where atmospheric saturation is otherwise expected. Winter water of this type is not seen in profiles from the Siberian Arctic (Bourgain & Gascard, 2011; Janout et al., 2017) or in the Eurasian Basin of the Arctic Ocean, including along the Transpolar Drift (Rabe et al., 2022) which means that these are an unlikely source. A similar water type is observed in the Wandel Sea at the deeper depth of 80 m (Dmitrenko et al., 2017). Ob bank is shallow (50 m) and, although absent in 2017, frequently obstructed by an ice barrier which would modify any water advected via this route. We subsequently conclude the water must therefore be advected from the east or be formed locally.

The NGWW is absent only in the Offshelf group where mixing occurs directly between the sea ice influenced surface and the Atlantic influenced water types. This implies that sea ice is melting directly into RAW and there is low to no remote riverine contribution at these CTD station locations. Additionally, the LHW is absent for these stations indicating that this water has not experienced the required conditions for it to be formed, for example, the entrainment of Atlantic water into a low salinity mixed layer and subsequent cooling (Rudels, 2021). This suggests that this is unmodified RAW.

The UHW is absent from our data and based on the N:P ratio the presence of Pacific water is unlikely. Rather, the geochemical tracers indicate that the entire cold halocline layer is composed of Atlantic water which is both diluted by river discharge and influenced by brine extrusion due to sea ice freezing. The TA:S (Figure 6a) and $\delta^{18}\text{O}$:S (Figure 6b) show that the Pacific end-member falls on the mixing lines for the Kolyma (TA:S) and the Yenisey/Mackenzie ($\delta^{18}\text{O}$:S) rivers and therefore cannot be used to identify Pacific water or even the primary meteoric river source. This has previously been observed and commented on (Forryan et al., 2019). Care must be taken in the use of non-conservative tracers as is apparent from our N:P analysis. Be that as it may, the nutrients plotted against AOU (Figure 9) are surprisingly similar to the regression relationship found for the Laptev Sea, especially near the surface. Far more similar in fact than they are to these ratios for the East Siberian Sea, which is geographically closer to and downstream of the Laptev Sea, does contain Pacific water and may be entrained into the Transpolar drift. We therefore consider AOU plotted against nutrient ratios as tentative but weak additional evidence against Pacific water presence on the Northeast Greenland shelf in late summer 2017.

The slope of the $\delta^2\text{H}:\delta^{18}\text{O}$ relationships of the six major Arctic rivers are known to be unique to each river (Yi et al., 2012; Table 1). They provide a clue to the provenance of the meteoric water found on the Northeast Greenland shelf (Figure 8). The bulk of these data fall between the Lena River regression and the summer Arctic Meteoric Water Line (Mellat et al., 2021) for all salinities. We interpret the proximity of our data to the Lena river line from Yi et al. (2012) on the $\delta^2\text{H}:\delta^{18}\text{O}$ diagram as evidence of the presence of a detectable volume of Lena river water on the Northeast Greenland shelf. Some of the lowest isotopic values δ -values tend more toward the Global Meteoric Water Line. These datapoints have the lowest salinities. Discussing the deuterium excess is beyond the scope of this paper, however we tentatively suggest this is due to the increased influence of precipitation in the fresher water on the shelf.

Although more data is required to verify the connection, our data imply that a large fraction of the meteoric water on the Northeast Greenland shelf during August–September 2017 has its origin in the Laptev Sea and ultimately in the Lena River catchment area. This is in line with previous suggestions of a connection between Siberian rivers and freshwater provenance in Fram Strait (Dodd et al., 2012; Granskog et al., 2012) shown by isotopic and organic matter fluorescence tracing. Furthermore, the layer above the maximum winter mixed layer depth, the NGWW, is significantly influenced by sea ice melt and much fresher than it was in previous decades.

6. Conclusions

Our data suggest a complex hydrography for the Northeast Greenland shelf, with much of the freshwater contained at depths below the maximum winter mixed layer depth (NGWW) having its source in the Laptev Sea region of the Siberian Arctic. From there it is transported to Fram Strait by the Transpolar Drift and subsequently advected onto the shelf. The freshwater shows a geochemical signature typical of that area, mixing along a line from brine-enhanced river discharge to Atlantic water. The Northeast Greenland Shelf lacks both Pacific water and UHW biogeochemical signatures in late summer 2017.

The NGWW is interpreted as the remnant of the previous seasons maximum winter mixed layer depth due to similarities with such winter mixed layer remnants elsewhere in the Arctic. The unique high oxygen saturation in the upper part of the remnant winter mixed layer may be partially associated with export during freezing but more data is required to verify this since it may also result from primary productivity. This layer is much fresher now than it was two decades ago, which is evidence of climate-change induced Arctic freshening. The SW above the NGWW is strongly influenced by sea ice melt, which imposes its geochemical signature in TA and $\delta^{18}\text{O}$ and possibly in the relatively low surface dissolved oxygen saturation.

The supply of freshwater to the Northeast Greenland shelf will likely increase in the following decades due to increases in discharge from the Siberian rivers and the Greenland Ice Sheet, and sea ice melt. If the Atlantic inflow continues to warm and return Atlantic flow remains available along the slope, the difference between on- and off-shelf water masses will increase. Mixing processes along the slope and LHW erosion may be enhanced consequently.

Data Availability Statement

All hydrographic and sample data can be found in the Pangaea repository at <https://doi.pangaea.de/10.1594/PANGAEA.956318>. Comparative data and relationships from literature are shown and referenced in Table 1.

References

- Aksenov, Y., Karcher, M., Proshutinsky, A., Gerdes, R., de Cuevas, B., Golubeva, E., et al. (2016). Arctic pathways of Pacific water: Arctic Ocean Model Intercomparison experiments. *Journal of Geophysical Research: Oceans*, *121*(1), 27–59. <https://doi.org/10.1002/2015JC011299>
- Alkire, M. B., Rember, R., & Polyakov, I. (2021). The Pacific-Atlantic front in the east Siberian Sea of the Arctic Ocean. In *The Handbook of Environmental Chemistry*. Springer. https://doi.org/10.1007/978_2021_795
- Anderson, L. G., Andersson, P. S., Björk, G., Peter Jones, E., Jutterström, S., & Wählström, I. (2013). Source and formation of the upper halocline of the Arctic Ocean. *Journal of Geophysical Research: Oceans*, *118*(1), 410–421. <https://doi.org/10.1029/2012JC008291>
- Arndt, J. E., Jokat, W., Dorschel, B., Myklebust, R., Dowdeswell, J. A., & Evans, J. (2015). A new bathymetry of the Northeast Greenland continental shelf: Constraints on glacial and other processes. *Geochemistry, Geophysics, Geosystems*, *16*(10), 3733–3753. <https://doi.org/10.1002/2015gc005931>
- Bauch, D., Dmitrenko, I. A., Wegner, C., Hölemann, J., Kirillov, S. A., Timokhov, L. A., & Kassens, H. (2009). Exchange of Laptev Sea and Arctic Ocean halocline waters in response to atmospheric forcing. *Journal of Geophysical Research*, *114*(C5), C05008. <https://doi.org/10.1029/2008jc005062>
- Bauch, D., van der Loeff, M. R., Andersen, N., Torres-Valdes, S., Bakker, K., & Abrahamson, E. P. (2011). Origin of freshwater and polynya water in the Arctic Ocean halocline in summer 2007. *Progress in Oceanography*, *91*(4), 482–495. <https://doi.org/10.1016/j.pocan.2011.07.017>
- Bezanson, J., Edelman, A., Karpinski, S., & Shah, V. B. (2017). Julia: A fresh approach to numerical computing. *SIAM Review*, *59*(1), 65–98. <https://doi.org/10.1137/141000671>
- Bignami, F., & Hopkins, T. S. (1997). The water mass characteristics of the Northeast Water polynya: Polar Sea data 1992–1993. *Journal of Marine Systems*, *10*(1–4), 139–156. [https://doi.org/10.1016/S0924-7963\(96\)00079-6](https://doi.org/10.1016/S0924-7963(96)00079-6)
- Bourgain, P., & Gascard, J. C. (2011). The Arctic Ocean halocline and its interannual variability from 1997 to 2008. *Deep Sea Research Part I: Oceanographic Research Papers*, *58*(7), 745–756. <https://doi.org/10.1016/j.dsr.2011.05.001>
- Budéus, G., & Schneider, W. (1995). On the hydrography of the Northeast Water polynya. *Journal of Geophysical Research*, *100*(C3), 4287. <https://doi.org/10.1029/94jc02024>
- Budéus, G., Schneider, W., & Kattner, G. (1997). Distribution and exchange of water masses in the Northeast Water polynya (Greenland Sea). *Journal of Marine Systems*, *10*(1), 123–138. [https://doi.org/10.1016/S0924-7963\(96\)00074-7](https://doi.org/10.1016/S0924-7963(96)00074-7)
- Charette, M. A., Kipp, L. E., Jensen, L. T., Dabrowski, J. S., Whitmore, L. M., Fitzsimmons, J. N., et al. (2020). The Transpolar drift as a source of riverine and shelf-derived trace elements to the central Arctic Ocean. *Journal of Geophysical Research: Oceans*, *125*(5). <https://doi.org/10.1029/2019JC015920>
- Codispoti, L. A., Friederich, G. E., Sakamoto, C. M., & Gordon, L. I. (1991). Nutrient cycling and primary production in the marine systems of the Arctic and Antarctic. *Journal of Marine Systems*, *2*(3–4), 359–384. [https://doi.org/10.1016/0924-7963\(91\)90042-S](https://doi.org/10.1016/0924-7963(91)90042-S)
- Cooper, L. W., Cota, G. F., Pomeroy, L. R., Grebmeier, J. M., & Whitedge, T. E. (1999). Modification of NO, PO, and NO/PO during flow across the Bering and Chukchi shelves: Implications for use as Arctic water mass tracers. *Journal of Geophysical Research*, *104*(C4), 7827–7836. <https://doi.org/10.1029/1999JC900010>
- Cooper, L. W., McClelland, J. W., Holmes, R. M., Raymond, P. A., Gibson, J. J., Guay, C. K., & Peterson, B. J. (2008). Flow-weighted values of runoff tracers ($\delta^{18}\text{O}$, DOC, Ba, alkalinity) from the six largest Arctic rivers. *Geophysical Research Letters*, *35*(18), L18606. <https://doi.org/10.1029/2008gl035007>

Acknowledgments

We would like to thank two anonymous reviewers for providing detailed and relevant feedback and making a positive contribution to this manuscript. The cruises were funded through the Greenland Ecosystem Monitoring Program (Leg 1), the Danish Centre for Marine Research, the Natural Sciences and Engineering Research Council of Canada (NSERC), and the Independent Research Fund Denmark (G-Ice Project) (Grant 7014-00113B/FNU) (Leg 2). This study received financial support from the Aage V Jensens Foundation, the Arctic Research Centre, Aarhus University, and Independent Research Fund Denmark (GreenShelf project (Grant 0135-00165B/FNU) to MSS). The captain and crew of RV DANA are acknowledged for excellent assistance during our field cruise to NE Greenland. Egon Frandsen is acknowledged for support on logistics and operations.

- Craig, H. (1961). Isotopic variations in meteoric waters. *Science*, 133(3465), 1702–1703. <https://doi.org/10.1126/science.133.3465.1702>
- Dmitrenko, I. A., Kirillov, S. A., Rudels, B., Babb, D. G., Pedersen, L. T., Rysgaard, S., et al. (2017). Arctic Ocean outflow and glacier–ocean interactions modify water over the Wandel Sea shelf (northeastern Greenland). *Ocean Science*, 13(6), 1045–1060. <https://doi.org/10.5194/os-13-1045-2017>
- Dodd, P. A., Rabe, B., Hansen, E., Falck, E., Mackensen, A., Rohling, E., et al. (2012). The freshwater composition of the Fram Strait outflow derived from a decade of tracer measurements. *Journal of Geophysical Research*, 117(C11). <https://doi.org/10.1029/2012JC008011>
- Falck, E. (2001). Contribution of waters of Atlantic and Pacific origin in the Northeast Water polynya. *Polar Research*, 20(2), 193–200. <https://doi.org/10.3402/polar.v20i2.6517>
- Falck, E., Kattner, G., & Budéus, G. (2005). Disappearance of Pacific water in the northwestern Fram Strait. *Geophysical Research Letters*, 32(14). <https://doi.org/10.1029/2005gl023400>
- Feistel, R. (2012). TEOS-10: A new international oceanographic standard for seawater, ice, fluid water, and humid air. *International Journal of Thermophysics*, 33(8–9), 1335–1351. <https://doi.org/10.1007/s10765-010-0901-y>
- Foldvik, A., Aagaard, K., & Tjørresen, T. (1988). On the velocity field of the East Greenland Current. *Deep-Sea Research, Part A: Oceanographic Research Papers*, 35(8), 1335–1354. [https://doi.org/10.1016/0198-0149\(88\)90086-6](https://doi.org/10.1016/0198-0149(88)90086-6)
- Forryan, A., Bacon, S., Tsubouchi, T., Torres-Valdés, S., & Naveira Garabato, A. C. (2019). Arctic freshwater fluxes: Sources, tracer budgets and inconsistencies. *The Cryosphere*, 13(8), 2111–2131. <https://doi.org/10.5194/tc-13-2111-2019>
- Gran, G. (1952). Determination of the equivalence point in potentiometric titrations. Part II. *The Analyst*, 77(920), 661. <https://doi.org/10.1039/an9527700661>
- Granskog, M. A., Stedmon, C. A., Dodd, P. A., Amon, R. M. W., Pavlov, A. K., de Steur, L., & Hansen, E. (2012). Characteristics of colored dissolved organic matter (CDOM) in the arctic outflow in the Fram Strait: Assessing the changes and fate of terrigenous CDOM in the Arctic Ocean. *Journal of Geophysical Research*, 117(C12). <https://doi.org/10.1029/2012jc008075>
- Haine, T. W. N., Curry, B., Gerdes, R., Hansen, E., Karcher, M., Lee, C., et al. (2015). Arctic freshwater export: Status, mechanisms, and prospects. *Global and Planetary Change*, 125, 13–35. <https://doi.org/10.1016/j.gloplacha.2014.11.013>
- Huhn, O., Rhein, M., Kanzow, T., Schaffer, J., & Sültenfuß, J. (2021). Submarine meltwater from Nioghalvfjærdsbræ (79 North Glacier), Northeast Greenland. *Journal of Geophysical Research: Oceans*, 126(7), e2021JC017224. <https://doi.org/10.1029/2021JC017224>
- Jakobsson, M., Mayer, L. A., Bringensparr, C., Castro, C. F., Mohammad, R., Johnson, P., et al. (2020). The international bathymetric chart of the Arctic Ocean version 4.0. *Scientific Data*, 7(1), 176. <https://doi.org/10.1038/s41597-020-0520-9>
- Janout, M. A., Hölemann, J., Timokhov, L., Gutjahr, O., & Heinemann, G. (2017). Circulation in the northwest Laptev Sea in the eastern Arctic Ocean: Crossroads between Siberian River water, Atlantic water and polynya-formed dense water. *Journal of Geophysical Research: Oceans*, 122(8), 6630–6647. <https://doi.org/10.1002/2017jc013159>
- Jones, E. P., & Anderson, L. G. (1986). On the origin of the chemical properties of the Arctic Ocean halocline. *Journal of Geophysical Research*, 91(C9), 10759. <https://doi.org/10.1029/jc091ic09p10759>
- Jones, E. P., Anderson, L. G., Jutterström, S., & Swift, J. H. (2008). Sources and distribution of fresh water in the East Greenland Current. *Progress in Oceanography*, 78(1), 37–44. <https://doi.org/10.1016/j.pocean.2007.06.003>
- Jones, E. P., Anderson, L. G., & Swift, J. H. (1998). Distribution of Atlantic and Pacific waters in the upper Arctic Ocean: Implications for circulation. *Geophysical Research Letters*, 25(6), 765–768. <https://doi.org/10.1029/98gl00464>
- Jones, E. P., Anderson, L. G., & Wallace, D. W. R. (1991). Tracers of near-surface, halocline and deep waters in the Arctic ocean: Implications for circulation. *Journal of Marine Systems*, 2(1–2), 241–255. [https://doi.org/10.1016/0924-7963\(91\)90027-R](https://doi.org/10.1016/0924-7963(91)90027-R)
- Kikuchi, T., Hatakeyama, K., & Morison, J. H. (2004). Distribution of convective lower halocline water in the eastern Arctic Ocean. *Journal of Geophysical Research*, 109(C12), C12030. <https://doi.org/10.1029/2003JC002223>
- Lansard, B., Mucci, A., Miller, L. A., Macdonald, R. W., & Gratton, Y. (2012). Seasonal variability of water mass distribution in the southeastern Beaufort Sea determined by total alkalinity and $\delta^1\text{O}$: Water masses in the Beaufort Sea. *Journal of Geophysical Research*, 117(C3). <https://doi.org/10.1029/2011JC007299>
- Lin, P., Pickart, R., Heorton, H., Tsamados, M., Itoh, M., & Kikuchi, T. (2022). New State of the Arctic Ocean's Beaufort Gyre (preprint). *Review*. <https://doi.org/10.21203/rs.3.rs-1774491/v1>
- Mellat, M., Bailey, H., Mustonen, K.-R., Marttila, H., Klein, E. S., Gribanov, K., et al. (2021). Hydroclimatic controls on the isotopic ($\delta^{18}\text{O}$, $\delta^2\text{H}$, d-excess) traits of pan-Arctic summer rainfall events. *Frontiers of Earth Science*, 9, 651731. <https://doi.org/10.3389/feart.2021.651731>
- Moon, T. A., Gardner, A. S., Csatho, B., Parmuzin, I., & Fahnestock, M. A. (2020). Rapid reconfiguration of the Greenland ice sheet coastal margin. *Journal of Geophysical Research: Earth Surface*, 125(11). <https://doi.org/10.1029/2020jf005585>
- Namyatov, A. A. (2021). δO as a tracer of the main regularities of water mass mixing and transformation in the Barents, Kara, and Laptev seas. *Journal of Hydrology*, 593, 125813. <https://doi.org/10.1016/j.jhydrol.2020.125813>
- Nguyen, A. T., Kwok, R., & Menemenlis, D. (2012). Source and pathway of the Western Arctic upper halocline in a data-constrained coupled ocean and sea ice model. *Journal of Physical Oceanography*, 42(5), 802–823. <https://doi.org/10.1175/JPO-D-11-040.1>
- Nitshinsky, M., Anderson, L. G., & Hölemann, J. A. (2007). Inorganic carbon and nutrient fluxes on the Arctic Shelf. *Continental Shelf Research*, 27(10–11), 1584–1599. <https://doi.org/10.1016/j.csr.2007.01.019>
- O'Neil, J. R. (1968). Hydrogen and oxygen isotope fractionation between ice and water. *The Journal of Physical Chemistry*, 72(10), 3683–3684. <https://doi.org/10.1021/j100856a060>
- Osadchiev, A. A., Pisareva, M. N., Spivak, E. A., Shchuka, S. A., & Semiletov, I. P. (2020). Freshwater transport between the Kara, Laptev, and East-Siberian seas. *Scientific Reports*, 10(1), 13041. <https://doi.org/10.1038/s41598-020-70096-w>
- Paffrath, R., Laukert, G., Bauch, D., Rutgers van der Loeff, M., & Pahnke, K. (2021). Separating individual contributions of major Siberian rivers in the Transpolar drift of the Arctic Ocean. *Scientific Reports*, 11(1), 8216. <https://doi.org/10.1038/s41598-021-86948-y>
- Peralta-Ferriz, C., & Woodgate, R. A. (2015). Seasonal and interannual variability of pan-Arctic surface mixed layer properties from 1979 to 2012 from hydrographic data, and the dominance of stratification for multiyear mixed layer depth shoaling. *Progress in Oceanography*, 134, 19–53. <https://doi.org/10.1016/j.pocean.2014.12.005>
- QGIS Development Team. (2022). QGIS geographic information system (manual). Retrieved from <https://www.qgis.org>
- Rabe, B., Heuzé, C., Regnery, J., Aksenov, Y., Allerholt, J., Athanase, M., et al. (2022). Overview of the MOSAiC expedition: Physical oceanography. *Elementa: Science of the Anthropocene*, 10(1), 00062. <https://doi.org/10.1525/elementa.2021.00062>
- Rudels, B. (2021). *The physical oceanography of the Arctic Mediterranean sea: Explorations, observations, interpretations*. Elsevier.
- Rudels, B., Jones, E. P., Schauer, U., & Eriksson, P. (2004). Atlantic sources of the Arctic Ocean surface and halocline waters. *Polar Research*, 23(2), 181–208. <https://doi.org/10.3402/polar.v23i2.6278>
- Rysgaard, S., Glud, R. N., Sejr, M. K., Bendtsen, J., & Christensen, P. B. (2007). Inorganic carbon transport during sea ice growth and decay: A carbon pump in polar seas. *Journal of Geophysical Research*, 112(C3), C03016. <https://doi.org/10.1029/2006JC003572>

- Schauer, U., Rudels, B., Jones, E. P., Anderson, L. G., Muench, R. D., Björk, G., et al. (2002). Confluence and redistribution of Atlantic water in the Nansen, Amundsen and Makarov basins. *Annales Geophysicae*, 20(2), 257–273. <https://doi.org/10.5194/angeo-20-257-2002>
- Semiletov, I. (2005). The East Siberian Sea as a transition zone between Pacific-derived waters and Arctic shelf waters. *Geophysical Research Letters*, 32(10), L10614. <https://doi.org/10.1029/2005GL022490>
- Shiklomanov, A., Déry, S., Tretiakov, M., Yang, D., Magritsky, D., Georgiadi, A., & Tang, W. (2021). River freshwater flux to the arctic ocean. In D. Yang, & D. L. Kane (Eds.), *Arctic hydrology, permafrost and ecosystems* (pp. 703–738). Springer International Publishing. <https://doi.org/10.1007/978-3-030-50930-924>
- SmithIV, D. C., & Morison, J. H. (1998). Nonhydrostatic haline convection under leads in sea ice. *Journal of Geophysical Research*, 103(C2), 3233–3247. <https://doi.org/10.1029/97JC02262>
- Smith, W. O., & Barber, D. G. (Eds.). (2007). *Polynyas: Windows to the world*. Elsevier.
- Sneed, W. A., & Hamilton, G. S. (2016). Recent changes in the Norske Øer ice barrier, coastal Northeast Greenland. *Annals of Glaciology*, 57(73), 47–55. <https://doi.org/10.1017/aog.2016.21>
- Sun, X., Humborg, C., Mörth, C., & Brüchert, V. (2021). The importance of benthic nutrient fluxes in supporting primary production in the Laptev and East Siberian shelf seas. *Global Biogeochemical Cycles*, 35(7). <https://doi.org/10.1029/2020GB006849>
- Sutherland, D. A., Pickart, R. S., Peter Jones, E., Azetsu-Scott, K., Jane Eert, A., & Ólafsson, J. (2009). Freshwater composition of the waters off southeast Greenland and their link to the Arctic Ocean. *Journal of Geophysical Research*, 114(C5), C05020. <https://doi.org/10.1029/2008JC004808>
- Tanaka, T., Guo, L., Deal, C., Tanaka, N., Whitedge, T., & Murata, A. (2004). N deficiency in a well-oxygenated cold bottom water over the Bering Sea shelf: Influence of sedimentary denitrification. *Continental Shelf Research*, 24(12), 1271–1283. <https://doi.org/10.1016/j.csr.2004.04.004>
- Thibodeau, B., Bauch, D., & Voss, M. (2017). Nitrogen dynamic in Eurasian coastal arctic ecosystem: Insight from nitrogen isotope: Nitrogen cycle over arctic shelves. *Global Biogeochemical Cycles*, 31(5), 836–849. <https://doi.org/10.1002/2016gb005593>
- Yamamoto-Kawai, M., McLaughlin, F. A., Carmack, E. C., Nishino, S., & Shimada, K. (2008). Freshwater budget of the Canada basin, Arctic Ocean, from salinity, $\delta^{18}\text{O}$, and nutrients. *Journal of Geophysical Research*, 113(C1), C01007. <https://doi.org/10.1029/2006jc003858>
- Yi, Y., Gibson, J. J., Cooper, L. W., Hélie, J.-F., Birks, S. J., McClelland, J. W., et al. (2012). Isotopic signals (^{18}O , ^2H , ^3H) of six major rivers draining the pan-arctic watershed. *Global Biogeochemical Cycles*, 26(1). <https://doi.org/10.1029/2011gb004159>